Solar Energy Materials & Solar Cells 95 (2011) 398–403

Contents lists available at ScienceDirect

Solar Energy Materials & Solar Cells

journal homepage: www.elsevier.com/locate/solmat

Diagnostics of thin-film silicon solar cells and solar panels/modules with variable intensity measurements (VIM)

A.V. Shah [a,*], F. Sculati-Meillaud [a], Z.J. Berényi [b], O.M. Ghahfarokhi [a], R. Kumar [c]

[a] Ecole Polytechnique Fédérale de Lausanne (EPFL), Institute of Microengineering (IMT), Photovoltaics and thin film electronics Laboratory, Breguet 2, 2000 Neuchâtel, Switzerland
[b] Energosolar, Szép u. 2, 1053 Budapest, Hungary
[c] HHV Solar Technologies Private Limited, Site No. 17, Phase 1, Peenya Industrial Area, Bangalore-560 058, India

ARTICLE INFO

Article history:
Received 7 November 2009
Received in revised form
24 February 2010
Accepted 16 April 2010
Available online 18 May 2010

Keywords:
Amorphous silicon
Modules
Diagnostics

ABSTRACT

A simple and low-cost method for analyzing amorphous silicon solar cells and modules, which have low values of the fill factor (*FF*), is proposed. Low fill factors can occur mainly because of 3 reasons: (a) excessive recombination due to "bad" intrinsic layers; (b) shunts and (c) very high series resistance. The method described here allows one to discriminate between (a), (b) and (c). It consists of measuring the *J*–*V* curves at different light intensities, varying typically from 0.05 to 1 sun. It has been called the "variable intensity method (VIM)". Here, one plots $R_{sc}=\partial V/\partial J$ (at $V=0$) and $R_{oc}=\partial V/\partial J$ (at $J=0$) as a function of J_{sc}. From the slope of the R_{sc}–J_{sc} curve, one derives the "collection voltage V_{coll}"; from the asymptotic value of R_{sc} for low values of J_{sc} (<0.1 mA/cm^2) one obtains the "true" shunt resistance R_{shunt}; from the asymptotic value of R_{oc} for high values of J_{sc} (around 10 mA/cm^2) one obtains the "true" series resistance R_{series}. This paper shows quantitatively how too low values of V_{coll} and of R_{shunt} as well as how too high a value of R_{series} lead to a low value of *FF* for both cells and panels/modules.

1. Introduction

A common task faced by both R and D laboratories and industries is to analyze why a cell or panel/module does not perform according to expectations. In general, this means that the conversion efficiency will be too low—so that either the short-circuit current density J_{sc}, the open-circuit voltage V_{oc} or the fill factor (*FF*) (or a combination of these 3 key solar cell parameters) is lower than what it should be. In the present paper we shall look at the case where the fill factor (*FF*) is too low. This is actually the most common case encountered.

The treatment given in this paper is based on variable intensity measurements (VIM) and on an "extended equivalent circuit" for solar cells [1]. The advantage of the VIM technique is that it is very inexpensive and that it can be used both at the cell and at the panel/module level. It is, indeed, common testing practice to compare the performance of cells and panels/modules at 1 sun with their performance at low light levels (0.01 suns), in order to detect shunts and to separate the shunt resistance generally used in the solar cell equivalent circuit into "dark shunts" (actual physical shunts) and "photo-shunts" (representing the effect of recombination). In that sense the treatment given here does not really introduce a fundamentally new method. The treatment given here is, however, placed within a systematic framework and should therefore be easier to understand for the beginner; it has, furthermore, the advantage of giving precise quantitative results whereas the test methods generally used so far just gave a qualitative "alert". Note that the VIM method and the corresponding "extended equivalent circuit" have already been used in their present form for microcrystalline silicon solar cells [2].

2. "Theoretical" calculations

2.1. Individual single-junction cells

2.1.1. Equivalent circuit

In order to enumerate the possible deficiencies, which may lead to low values of *FF*, we shall look at the equivalent circuit of Fig. 1, taken from [1]. The equivalent circuit of Fig. 1 is too complicated for use in electrical system design; on the other hand, it is very useful for cell diagnostics because it splits up the parallel resistance R_p of the usual equivalent circuit into two distinct parts: a recombination part (represented by J_{rec}) and "true" physical shunts (represented by R_{shunt}). Merten et al. [1] showed that there are over 5 decades of light intensity, an excellent fit between *J*–*V* curves calculated from this model and experimental *J*–*V* characteristics for typical a-Si:H solar cells. In the present paper, the equivalent circuit of Fig. 1 is utilized to describe the performance of a-Si:H solar cells and modules. The following types of defects can occur:

* Corresponding author. Tel.: +41 32 718 3209; fax: +41 32 718 3201.
E-mail address: arvind.shah@unine.ch (A.V. Shah).

0927-0248/$ - see front matter © 2010 Elsevier B.V. All rights reserved.
doi:10.1016/j.solmat.2010.04.070

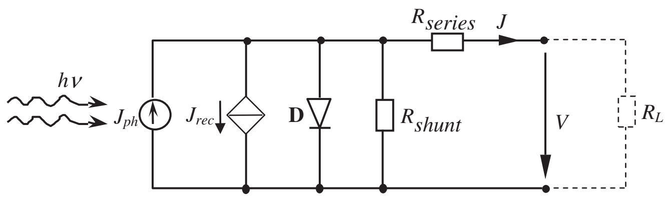

Fig. 1. Equivalent circuit for p–i–n-type solar cells [1]; the controlled current sink J_{rec} (Eq. (4)) depends on i-layer "quality", R_{shunt} originates from micro-shunts at the edges or in the bulk of the cell; R_{series} is given by contacts and TCO; the diode D is represented by Eq. (2), and characterized by J_o and n, where n is the diode ideality factor; J_o the diode reverse saturation current, which, in turn, is given by material band gap, defect density N_{defect} and by i-layer thickness d_i; and R_L is the load resistance.

(a) High value of J_{rec}, due e.g. to poor quality of i-layer.
(b) Low value of R_{shunt}, due to shunts formed e.g. because of lack of cleanliness in fabrication.
(c) High value of R_{series}, due e.g. to poor quality of TCO layers.

2.1.2. *Model for single-junction a-si:H solar cells*

The model used by us to describe amorphous silicon (a-Si:H) solar cells is based on adding collection current density J_{coll} and diode current density J_{diode} [2]:

$$J_{total} = J_{coll} + J_{diode} \tag{1}$$

J_{diode} is given by the drift-diffusion diode model

$$J_{diode} = J_o\{\exp(q\, V_{appl}/nkT)\text{-}1\} \tag{2}$$

for p–i–n diodes:

$$J_{coll} = J_{ph} - J_{rec} - J_{shunt} \tag{3}$$

with [1–3]:

$$J_{rec} = (d_i J_{ph})/(E_{eff}\,\mu\tau_{eff}) \tag{4}$$

Here, J_{ph} is the photogenerated current density; J_{rec} is the recombination current density; $J_{shunt}=V_{appl}/R_{shunt}$ is the current density through physical shunts; $\mu\tau_{eff}$ is the effective mobility times lifetime product of the i-layer; $E_{eff}=\{(V_{bi}-V_{appl})/\psi d_i\}$ is the effective electric field within the i-layer[1] ; d_i is the i-layer thickness; V_{bi} is the built-in voltage; V_{appl} is the external applied voltage; q is the unit charge; k the Boltzmann constant and T is the absolute temperature. E_{eff} is reduced by space charge: by ionized contaminants (O, B) and charged defects. At $V_{appl}=0$, we can write Eq. (4) in a different form:

$$J_{rec}\Big|_{V_{appl}=0} = J_{ph}(V_{bi}/V_{coll}) \tag{5}$$

with

$$V_{coll} = \frac{(\mu\tau)_{eff}\cdot V_{bi}^2}{d_i^2} \tag{6}$$

V_{coll} is an important quantity for analyzing the performance of thin-film silicon solar cells [2,3]; it is called the "*collection voltage*".

In accordance with [1], let us now introduce the "short-circuit resistance"[2] R_{sc}:

$$R_{sc} = (\partial V/\partial J)_{V=0} \tag{7}$$

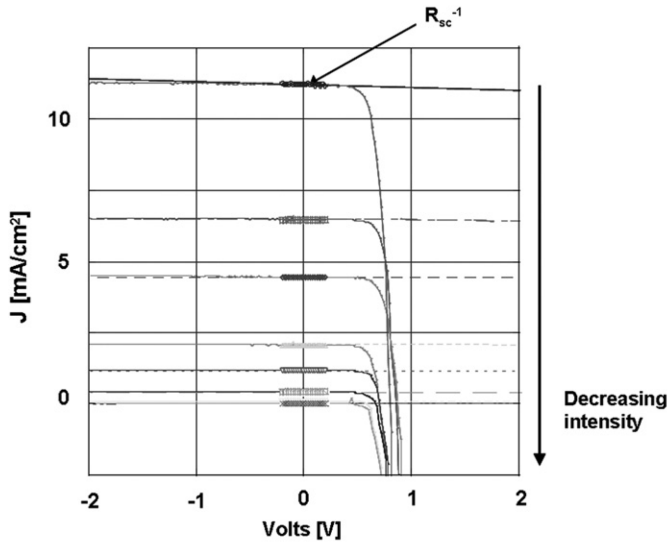

Fig. 2. Typical J–V curves of an amorphous silicon solar cell for different light intensities; the slope of the J–V curve at $V_{appl}=0$ is the reciprocal of the short-circuit resistance R_{sc}: the value of R_{sc} tends toward the value of the shunt resistance R_{shunt}, for low illumination intensities [1,3].

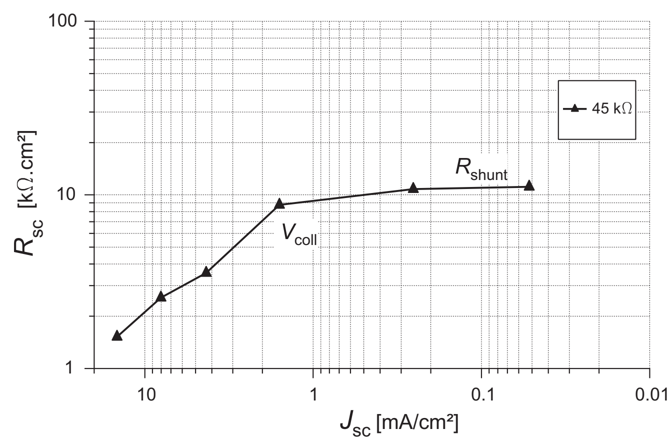

Fig. 3. Short-circuit resistance R_{sc} as a function of the reciprocal of the short-circuit current density $J_{sc}{}^{-1}$ for a typical a-Si:H solar cell; one clearly distinguishes two parts: on the left (for high light intensities), the curve for $R_{sc}(J_{sc}{}^{-1})$ is governed by the collection voltage, according to Eq. (8); on the right (for low light intensities) curve for $R_{sc}(J_{sc}{}^{-1})$ tends asymptotically towards R_{shunt}.

Hereafter R_{sc} corresponds, thus, to the inverse of the slope of the J–V curve at $V=0$ as shown in Fig. 2. By combining Eqs. (1) and (7), we establish that the collection voltage V_{coll} can be experimentally assessed from measurements of R_{sc} as a function of $J_{sc}^{-1}(\approx J_{ph}^{-1})$:

$$R_{sc} = V_{coll}/J_{sc} \tag{8}$$

This is illustrated by Fig. 3.

2.1.3. *Analyzing the fill factor (FF) [4]*

For a-Si:H solar cells, the "ideal" value of FF is well over 75%; however, in practice, cells often exhibit values in the range 60–70%. In thin-film silicon solar cells, there are 3 main reasons why FF is reduced to values below its limit value: (a) recombination losses within the i-layer and at the p/i and i/n interfaces; (b) partial micro-shunts through the i-layer (and through the whole cell) and (c) contact and doped layers with too high resistivity. In the equivalent circuit of Fig. 1, effect (a) increases

[1] Ψ is a correction factor taking into account the deformation of electric field $E(x)$. We will consider it to be 1 in the following development. This is probably verified in thin a-Si:H solar cells ($d_i<250$ nm); in thicker cells ($d_i=400$ nm), we probably have $\Psi=2$ [2,3].

[2] Note that all resistance values given in this paper are "specific resistances" i.e., they are multiplied with the corresponding cell area, their unit is $\Omega\,\text{cm}^2$. This is in accordance with the general use of "current densities J" rather than of "currents I".

J_{rec} by decreasing the collection voltage $V_{coll} = \mu\tau_{eff} \times (V_{bi}/\psi d_i)$; effect (b) decreases R_{shunt} and effect (c) increases R_{series}.

In practice it is important to analyze why the *FF* of a given cell is low. Here, VIM-analysis can help:

- Plot log $R_{sc} = f\{\log(J_{sc}^{-1})\}$, as in Fig. 3 (for the definition of $1/R_{sc}$, see Fig. 2).
- The slope of the log R_{sc} curve is, at high light intensities, indeed equal to V_{coll}.
- The curve itself goes asymptotically towards R_{shunt}, for $J_{sc} \to 0$.
- The curve itself goes, in principle, asymptotically towards R_{series}, for $J_{sc} \to \infty$. but this asymptote is difficult to reach, because very high light intensities (> 1 sun) cannot be used in the case of a-Si:H solar cells.

2.1.3.1. FF-reduction for increased recombination. Let us exemplify this situation by looking at a-Si:H cells that undergo light-induced degradation. Thereby we assume that V_{oc} and J_{sc} remain unchanged. This is shown schematically in Fig. 4. We thereby note the following points:

I. The maximum power point (MPP) is always at approximately the same voltage V_{MPP};
II. $V_{MPP} \approx 0.7 \cdot$ and $V_{bi} \approx 0.7$ V (we assume $V_{bi} \approx 1$ V for a-Si:H);
III. in the ideal case J_{rec} can be neglected, i.e. $J_{sc} = J_{ph}$;
IV. $V_{MPP} \approx 0.9$ V_{oc} (as experimentally observed);
V. $J_{MPP,\ ideal} \approx 0.8 J_{sc}$ (as experimentally observed);
The assumptions from I to V lead to
VI. $J_{MPP,\ ideal} - J_{MPP,\ degraded} = \Delta J_{MPP} = J_{rec,\ degradation}$

Now, with FF_0 equal to the highest measured *FF* in our lab (77%), we obtain from (5) and (7) that

$$\Delta FF = FF_0 - FF_{\text{degraded}} = \frac{V_{MPP}\Delta J_{MPP}}{J_{sc}V_{oc}} = \frac{J_{rec,deg}}{J_{sc}}\frac{V_{MPP}}{V_{oc}} \approx 0.9\frac{J_{rec,deg}}{J_{sc}} \tag{9}$$

By combining Eqs. (1) and (2), we can write

$$\Delta FF \approx 0.9\frac{d_i^2}{(\mu^0\tau^0)_{\text{degraded}}(V_{bi} - V_{MPP,\text{degraded}})} \tag{10}$$

and with the assumption (II) we obtain (with d_i^2 in cm^2 and $\mu^0\tau^0$ in cm^2/V):

$$FF_0 - FF_{\text{degraded}} \approx 1.8\frac{d_i^2}{(\mu^0\tau^0)_{\text{degraded}}} = 180\%\frac{d_i^2}{(\mu^0\tau^0)_{\text{degraded}}} \tag{11}$$

If we now look at the collection voltage V_{coll}, we find from Eqs. (2) and (9):

$$FF_0 - FF_{\text{degraded}} \approx \frac{V_{bi}}{V_{coll}}\frac{V_{MPP}}{V_{oc}} \approx \frac{V_{bi}}{V_{coll}} 90\% \tag{12}$$

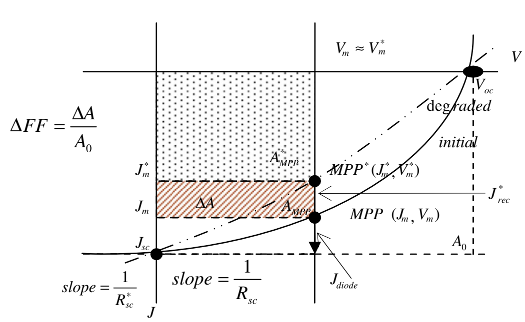

Fig. 4. Schematic representation of *J–V* curves for ideal cell and cell with strong recombination losses J_{rec}.

or:

$$\Delta FF \approx \frac{V_{bi}}{V_{coll}} 90\% \tag{13}$$

with $V_{bi} \approx 1$ V and V_{coll} that can be directly obtained from VIM measurements.

We suggest that the above relationship can be used, as a "general guideline" to evaluate roughly to what extent a low value of V_{coll} will affect the *FF* of a solar cell, not only for the case of light-induced degradation but also for other cases, where the band gap of the material remains unchanged and the recombination increases due to increased defect density. Indeed, according to Eq. (6), V_{coll} is proportional to $\mu\tau_{eff} \times E^0_{eff}$, i.e. to the drift length L^0_{drift}prevailing in the *i*-layer for zero applied field; the internal electric field being then $E^0_{eff} \approx V_{bi}/d_i$. Thus, a low value of V_{coll} indicates, in all cases, a large amount of recombination.

Note: the determination of V_{coll} (by measuring *J–V* curves at different light intensities) is probably the easiest and most reliable way to evaluate the "quality" of the *i*-layer (of bulk and interfaces), within the completed cell. It is a convenient and easy way to obtain information about the drift length L^0_{drift}, i.e. about the key parameter governing all classical collection models [5–7] in the theory of amorphous silicon solar cells.

2.1.3.2. Partial shunting. From the equivalent circuit of Fig. 1 we obtain

$$\Delta J_{MPP} = \frac{V_{MPP}}{R_{shunt}} \tag{14}$$

and Eq. (9) becomes

$$\Delta FF = \frac{V_{MPP}\Delta J_{MPP}}{J_{sc}V_{oc}} = \frac{V_{MPP}}{J_{sc}}\frac{V_{MPP}}{V_{oc}}\frac{1}{R_{shunt}} \tag{15}$$

In state-of-the-art a-Si:H solar cells we have $V_{MPP}/J_{sc} \approx 0.05$ kΩ cm^2 ($V_{MPP} \approx 0.7$ V, $J_{sc} \approx 14.5$ mA/cm^2),

Eq. (15), thus, gives

$$\Delta FF \approx 4\%\frac{1}{R_{shunt}} \quad \text{with} \quad R_{shunt} \text{ in } k\Omega\text{cm}^2 \tag{16}$$

2.1.3.3. High series resistance. With similar considerations as under (b) we find

$$\Delta FF \approx 1.5\%\frac{1}{R_{series}} \quad \text{with} \quad R_{series} \text{ in } \Omega\text{cm}^2 \tag{17}$$

2.2. Entire panels and modules

The situation with entire panels/modules is more complex. In addition to all the deficiencies we have with individual solar cells (and which are described above), there are the following supplementary defects at the panel/module level:

(a) Additional shunts created by laser scribing and by edge machining (edge ablation/edge deletion).
(b) Additional series resistance due to unsatisfactory interconnection between individual cells.
In a first analysis we shall assume that we are dealing with modules, which have no such additional defects.

2.2.1. Panels/modules without additional defects at the panel/module level

Consider a panel/module, which is a series connection of *m* individual cells. Here, the whole panel/module behaves just like an individual cell with the following parameters:

$$V_{oc.panel} = \sum_{i=1}^{i=m} V_{oc.i} = m \times \overline{V}_{oc.cell} \tag{18}$$

$$J_{sc.panel} = \min(J_{sc.i}) = \min(J_{sc.cell}) \tag{19}$$

$$FF_{panel} = f(FF_i) = f(FF_{cell}) \tag{20}$$

and

$$R_{sc.panel} = \sum_{i=1}^{i=m} R_{sc.i} = m \times \overline{R}_{sc.cell} \tag{21}$$

$$R_{oc.panel} = \sum_{i=1}^{i=m} R_{oc.i} = m \times \overline{R}_{oc.cell} \tag{22}$$

where the symbols used are self-evident.

The VIM-analysis can be carried out on the panel/module, in exactly the same way as with the individual cell, except that the *FF*-reduction factors will now read:

$$\{(mV_{bi}/V_{coll}) \times 90\%\}; \{1.5/\mathrm{mR}_{\mathrm{series}}\}; \{4 \times (1/mR_{shunt})\} \tag{23}$$

where R_{series} is to be given in $\Omega\,\mathrm{cm}^2$ and R_{shunt} in $\mathrm{k}\Omega\,\mathrm{cm}^2$.

2.2.2. Remarks on effect of shunts on module performance

If we are dealing with individual cells, a shunt will always have a direct effect on the *FF*; it will also be clearly visible in VIM-curves. For panels/modules the situation is somewhat different: imagine that one of the totally *m* cells is shunted or, even better, completely short-circuited. The corresponding cell is, in the latter case, so to say simply "replaced by a wire". It is, thus, evident that such a short-circuit has absolutely no effect on the *FF* of the entire panel/module; it will simply lead to a reduction of the V_{oc}-value of the entire panel/module from $m \times \overline{V}_{oc.cell}$ to $(m-1) \times \overline{V}_{oc.cell}$. In practice such a situation will rarely arise. In fact, shunts generally fall into one of the following categories:

(1) Shunts due to insufficient substrate cleaning; dust in the fabrication; powder in the PE-CVD reactors → this leads usually already to shunts at the level of the individual cells.
(2) Shunts due to laser scribing → this leads to many shunts distributed over the whole surface of the panel/module.
(3) Shunts due to machining of panels/modules (edge deletion, etc.) → this leads to shunts concentrated in the corresponding areas of the module.
(4) Shunts due to damage of the panel/module by bad handling (after fabrication) → this may indeed lead to a single shunt on one of the cells only. It is, however, the only case where such a phenomenon, in which only a single cell is shunted, is likely to occur.

The VIM technique does not help us to distinguish between the different categories (1)–(4) of shunts. For that purpose one must use an imaging technique, such as lock-in thermography.

2.2.3. Case of additional shunting

If additional shunts occur at the panel/module level (and this is indeed a case, which is very likely in practice), we can, according to the theorems of linear circuit theory, still represent the entire panel/module with the equivalent circuit of Fig. 1. We will now be having a reduction of the fill factor *FF*, which can still be related to the global value of shunt resistance R_{shunt}, which can be found by performing VIM-analysis (as shown in Fig. 3) on the entire module.

2.3. Tandem cells and panels/modules with tandem cells

This is an additional complication. Basically, VIM-analysis can still be used, but the *FF*-reduction factors given in Eqs. (13)–(15) and relating to the effect of R_{series} and of R_{shunt} will have to be adjusted. For a situation with tandem cells, it is of special interest to find out which one of the 2 sub-cells forming the tandem is shunted; for this task VIM is not the suitable tool, and a measurement of the external quantum efficiency (EQE) curve (as a function of wavelength) is indicated. We shall not go into this topic in more detail, in the present paper.

3. Experimental

Cells/modules were fabricated and tested at 3 locations: (1) IMT Neuchâtel; (2) Energosolar, Budapest and (3) HHV Solar, Bangalore. Cells/modules reported here are not typical of current production techniques and results at these 3 facilities, but were specially selected because they exhibited the deficiencies described in this paper.

3.1. Cell/module structure and fabrication:

(1) IMT's cells are single-junction amorphous silicon cells of approximately $0.4\,\mathrm{cm}^2$ size, with the deposition sequence glass/LP-CVD ZnO/$\langle p \rangle$ a-Si,C:H/$\langle i \rangle$a-Si:H/$\langle n \rangle$a-Si:H/LP-CVD ZnO/dielectric reflector. They were deposited by VHF-GD in a multi-chamber parallel plate laboratory reactor.
(2) Energosolar's modules are composed of a-Si,C:H/a-Si:H tandem cells deposited on commercial SnO_2-clad glass plates; they contain 39 cells of $184\,\mathrm{cm}^2$ each; total module size is $1245 \times 635\,\mathrm{mm}^2$. Deposition is done in a single-chamber commercial production line at 13.56 MHz plasma excitation frequency.
(3) HHV's cells are single-junction a-Si:H cells, of approximately $1\,\mathrm{cm}^2$ size deposited on commercial SnO_2-clad glass plates. Deposition is done in a multi-chamber laboratory reactor at 13.56 MHz plasma excitation frequency.

3.2. Measurement/testing

(1) At IMT, a WACOM solar simulator and a commercial *J–V* tester were used. Variable intensity was obtained with the help of grey filters.
(2) At Energosolar, a multiflash-tester was used. Each flash provides for the time-resolved measurement of module current and irradiation; *k*-irradiation varies between 0 and $1600\,\mathrm{W/m}^2$; *J–V* curves are composed at 15 different irradiation levels between 15 and $1500\,\mathrm{W/m}^2$.
(3) At HHV a steady-state WACOM solar simulator and a commercial *J–V* tester were used. Variable intensity was obtained by interposition of *m* paper sheets of varying thicknesses.

4. Results and discussion

As first series of measurements, we show, in Fig. 5, the results of a light-induced degradation (LID) experiment performed on 4 cells from IMT. The LID experiment was not performed under standard degradation conditions, but designed to obtain an increase in defect density, such that the fill factor of the cells decreased by about 5%, within a relatively short time (10 h). A table lamp with a fluorescent "economy" bulb was used and the cells were placed directly under the bulb at a distance of about 5 cm. One notes that Eq. (10) is nicely verified.

As second series of measurements, external shunt resistances with values from 5.6 MΩ down to 1 kΩ were added, as parallel resistances to the solar cell, at IMT, simulating thereby the occurrence of shunting conditions. Fig. 6 shows the corresponding VIM diagrams. The possibility to detect and quantify shunts by VIM-analysis is thereby clearly demonstrated.

As third experiment, an external series resistance of 12 Ω was added to a cell fabricated at HHV. It was noted that the usual VIM diagram of log $R_{sc}=f\{\log(J_{sc}^{-1})\}$ does not show any effect of this series resistance. Therefore, the corresponding diagram for $R_{oc}=(\partial V/\partial J)_{J=0}$ was drawn (Fig. 7). The effect of the 12 Ω series resistance barely shows up at the left bottom corner of the diagram, i.e. for high light intensities. This shows that the VIM method is not a suitable tool for analyzing problems with series resistance at the cell level. At the module level the situation will be different, as will be shown hereunder.

A fourth series of experiments was performed on entire modules at Energosolar, on entire modules: Fig. 8 shows the effect of light-induced degradation on a typical module; the collection voltage V_{coll} decreases thereby from 27.4 to 15 V and *FF* decreases from 67% to 56%. Fig. 9 shows the effect of shunting: the VIM diagrams of 2 modules are shown, one of which exhibits pronounced shunting. Fig. 10 shows the effect of series resistance (within the modules): the VIM diagrams for R_{oc} are shown for 3 modules: one with a reasonably good value if series resistance and 2 with high series resistance. We note that VIM diagrams are useful tools for identifying and quantifying series resistance problems at the module level, provided one plots R_{oc} and not R_{sc}.

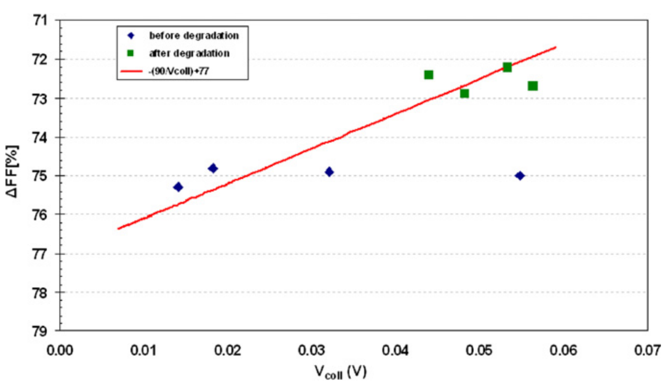

Fig. 5. Graph showing values for collection voltage V_{coll} and fill factor reduction ΔFF (in%) for 4 cells deposited at IMT Neuchâtel and having undergone 10 h of light-induced degradation.

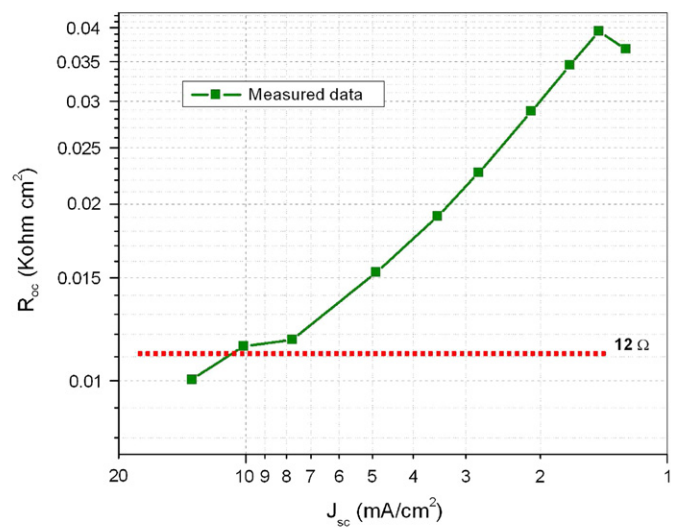

Fig. 7. VIM measurements on a cell from HHV, Bangalore, showing the influence of an external series resistance of 12 Ω.

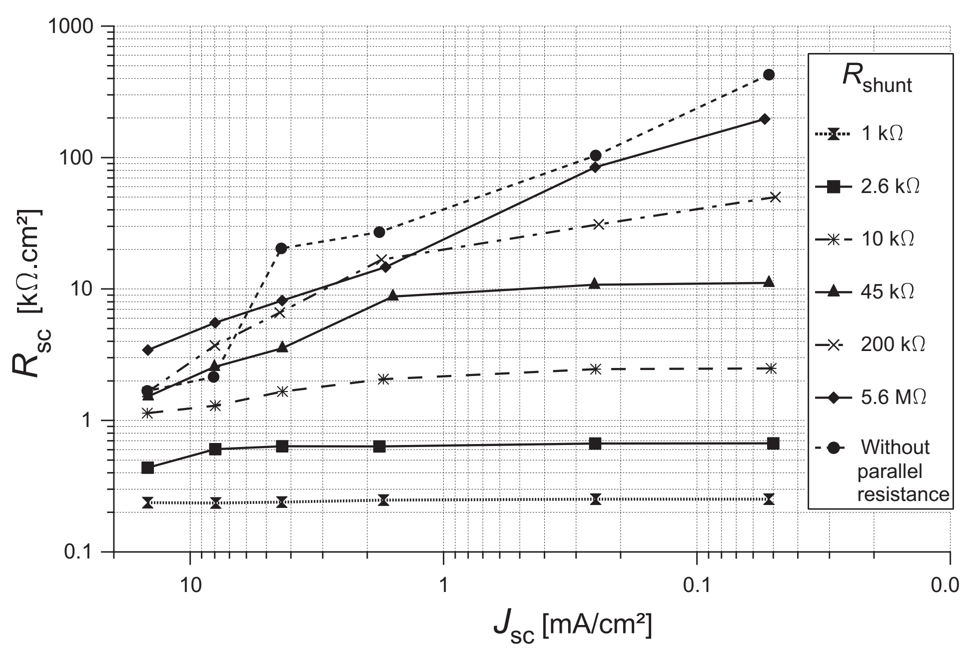

Fig. 6. VIM measurements on a cell from IMT Neuchâtel, with external shunt resistances, ranging from 5.6 MΩ down to 1 kΩ.

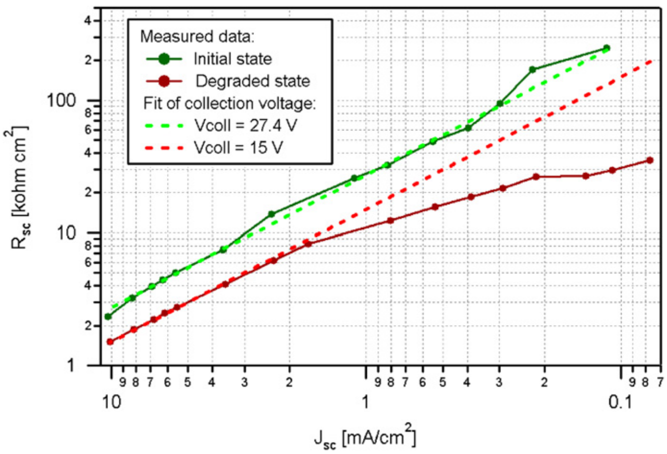

Fig. 8. VIM measurements on a module from Energosolar, Budapest showing the influence of light-induced degradation: the collection voltage V_{coll} decreases from 27.4 to 15 V and *FF* decreases from 67% to 56%.

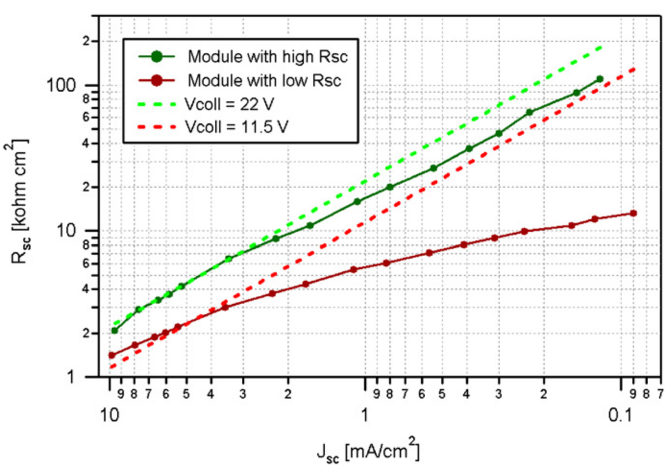

Fig. 9. VIM measurements on modules from Energosolar, Budapest showing the influence of shunting.

5. Conclusions

J–V curves provide a surprising amount of information on amorphous silicon solar cells and modules, provided one varies also the light intensity. One obtains information on (a) collection/recombination problems, on (b) shunting and (at least at the module level) and also on (c) problems of series resistance. The present paper is the first attempt to establish a systematic framework for such variable intensity measurements (VIM) in the case of amorphous silicon cells and modules.

The VIM method is, thus, destined to become a rapid and non-destructive screening method for identifying the problem pertaining to a defective cell or module. Thereby quantitative data on the deficiency are obtained. For individual single-junction cells, Table 1 indicates rough values for the fill factor losses that are obtained through the 3 types of deficiencies (a), (b) and (c) just mentioned, respectively.

Note, however, that VIM gives us only the first rapid screening and has to be followed up by other more specific techniques, such as EQE and SIMS for collection/recombination problems, lock-in thermography for shunting problems. For VIM to become really useful, much more measurement experience should be gained. This will be forthcoming if the VIM method is employed by various laboratories and, above all, by different module producers.

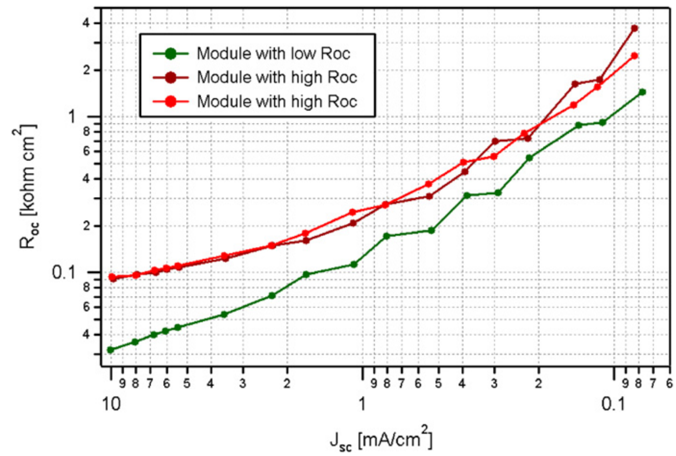

Fig. 10. VIM measurements on modules from Energosolar, Budapest showing the influence of series resistance.

Table 1
Common faults found on amorphous silicon solar cells and corresponding reduction of the fill factor, for the single-junction individual cells.

Fault	Measured parameter	*FF*-reduction (single-junction amorphous silicon cells)
Collection problem	V_{coll} (V)	$(V_{bi}/V_{coll}) \times 90\%$
High series resistance	R_{series} (Ω cm^2)	$1.5 \times R_{series}$
Low parallel resistance	R_{shunt} (kΩ cm^2)	$4 \times (1/R_{shunt})$

Acknowledgements

The authors thank C. Ballif, R. Boomsma, S. Prasanth, K. Mohanachandran and C. Banerjee for encouragement and support. A. Billet deposited the samples at IMT Neuchâtel and deserves special acknowledgement.

References

[1] J. Merten, J.M. Asensi, C. Voz, A. Shah, R. Platz, J. Andreu, Improved equivalent circuit and analytical model for amorphous silicon solar cells and modules, IEEE Trans. Electron Devices 45 (1998) 423–429.
[2] F. Meillaud, A. Shah, J. Bailat, E. Vallat-Sauvain, T. Roschek, B. Rech, D. Didier, T. Söderström, M. Python, C. Ballif, Microcrystalline silicon solar cells: theory and diagnostic tools, in: Proceedings of the fourth WCPEC conference, Hawaii, USA, 2006, pp. 1572–1575.
[3] C. Hof, Thin-film solar cells of amorphous silicon: influence of *i*-layer material on cell efficiency, Ph.D thesis, University of Neuchâtel, UFO Atelier für Gestaltung & Verlag, Band 379, ISBN 3-930803-78-X, 1999.
[4] F. Sculati-Meillaud, Microcrystalline silicon solar cells: theory, characterization and diagnostics, Ph.D thesis, University of Neuchâtel, 2006.
[5] R.S. Crandall, Modeling of thin-film solar cells: uniform-field approximation, J. Appl. Phys. 54 (1983) 7176–7186.
[6] B. Rech Ph.D Thesis, Forschungszentrum, Jülich, 1997.
[7] J. Hubin, A. Shah, Effect of the recombination function on the collection in a p–i–n solar cell, Phil. Mag. B 72 (1995) 589–599.